OPTIMISATION OF A DOMESTIC-SCALE SOLAR-ORC HEATING AND POWER SYSTEM FOR MAXIMUM POWER OUTPUT IN THE UK

James Freeman, Klaus Hellgardt and Christos N. Markides*

Clean Energy Processes (CEP) Laboratory, Department of Chemical Engineering, Imperial College London
South Kensington Campus, London SW7 2AZ, UK
e-mail: c.markides@imperial.ac.uk

* Corresponding Author

ABSTRACT

A model is presented of a domestic-scale solar combined heating and power (S-CHP) system, featuring an Organic Rankine Cycle (ORC) engine and a 15-m^2 solar-thermal collector array. The system is configured for operation in the UK, incorporating high-efficiency non-concentrating solar collectors and an ORC working fluid buffer vessel to maintain continuous electrical power output during periods of intermittent solar irradiance. The solar collector array configuration and choice of ORC working fluid are examined, and the system electrical performance is optimised over an annual period of operation by simulating with London UK climate data. By incorporating a two-stage solar collector/evaporator configuration, a maximum net annual electrical work output of 1070 kWh yr^{-1} (continuous power of 122 W) and a solar-to-electrical efficiency of 6.3% is reported with HFC-245ca as the ORC working fluid and an optimal evaporation temperature of 126 °C. This is equivalent to ~32% of the electricity demand of a typical (average) UK home, and represents an improvement of more than 50% over a recent effort by the same authors based on an earlier S-CHP system configuration and HFC-245fa.

1. INTRODUCTION

Solar energy has the potential to meet a significant proportion of household demands for heating and electricity in the UK, despite its comparatively low annual yield of incident solar radiation (~1000 kWh m^{-2} yr^{-1} for southern UK compared to ~1800 kWh m^{-2} yr^{-1} for parts of southern Europe). Distributed domestic solar-power provision is conventionally a choice of either electricity generation via photovoltaic (PV) devices, or water heating via solar-thermal collectors. The feasibility of installing these as side-by-side systems for provision of both heating and power is limited by cost and space availability. At present, the only available technologies that can provide both heating and power from the same area of solar collector array are hybrid PV-thermal (PVT) systems, which are expensive and have a limited ability to meet time-varying demand ratios for heating and power.

Organic Rankine cycle (ORC) systems are a promising alternative to PV-based technologies for electrical power generation from solar energy. The potential for solar-ORC systems to operate at lower temperatures and on smaller scales than solar-power systems based on steam-Rankine cycle technology opens up the possibility of developing the technology for geographical regions with a low solar resource and for distributed-level applications. Nonetheless, a significant amount of experimental and modelling research on these systems (Canada *et al*., 2004; Manolakos *et al*., 2009; Wang *et al*., 2009; Jing *et al*., 2010; Quoilin *et al*., 2011) have focused on application to regions with abundant solar resource and collector array areas beyond the size of what could be easily accommodated on the roof of a domestic property. The aim of this paper is to assess the electricity generating potential of an ORC-based solar combined heating and power (S-CHP) system when operating at lower solar irradiance levels and smaller scales, namely, at a northern European location (specifically, London, UK) and a domestic roof-sized installation.

In an earlier work (Freeman *et al*. 2015a), the authors presented a system model of a domestic-scale S-CHP system and simulated its performance in the UK climate. The system model featured a solar

collector array, a basic four-component (*non-regenerative*) ORC engine and a hot-water cylinder. Both the ORC engine and the hot-water cylinder received a thermal energy input from the solar collector array to meet a variable demand for heating and power. The ORC working fluid was the hydrofluorocarbon (HFC) refrigerant R245fa, also investigated for use in low-temperature solar-ORC systems by Wang *et al*., (2009) and Quoilin *et al*., (2011); and chosen for its low flammability and global warming potential, and also its low saturation temperature at atmospheric pressure. The system's fixed flow-rates and fixed operating temperatures and pressures were selected for maximum work production on an "annual-average" day and then simulated over an annual period.

It was found that the total electrical work output was 700 kWh yr^{-1} (80 W average), and that the whole system capital cost was between £4400-5500. However, the system was only crudely optimised and several potential areas for performance enhancement were identified. In this paper, a wider range of working fluids will be considered in order to find the optimum fluid to maximise annual work output from the system in the UK setting. The performance of a given working fluid is dependent upon the evaporation temperature of the Rankine cycle, which is itself dependent upon the choice of solar-thermal collector design and the solar irradiance characteristics of the chosen location. Consideration will also be given to system configurations that enable efficient operation of the solar collector array and continuous power output under intermittent solar irradiance conditions.

2. MODELLING METHODOLOGY

2.1 System description

A schematic diagram of the investigated system is shown in Figure 1a. Pump 1 is used to pressurise the working fluid from a saturated liquid at State 1 to its evaporation pressure at State 2a. The fluid is then preheated to State 2b in the regenerator heat-exchanger, before mixing with the saturated liquid stream from the buffer vessel circulated by Pump 2. The combined fluid-stream at State 2c enters the evaporator where it is heated by the solar-collector fluid circulated by Pump 3. Fluid leaving the evaporator at State 3a then proceeds to the buffer vessel. The buffer vessel is assumed to be held at a constant temperature equal to the evaporation temperature of the ORC, such that working fluid may be stored in a two-phase state within. A similar concept was proposed earlier, in the work by Jing *et al*. (2010), where it was suggested that the buffer vessel temperature could be maintained by conduits filled with phase change material (PCM). Saturated liquid from the buffer vessel is recycled to the evaporator by Pump 2, meanwhile saturated vapour from the buffer vessel (State 3b) proceeds on to the expander where it is expanded to the condensation pressure, producing shaft work. Low pressure vapour is exhausted from the expander (State 4a) and cooled (de-superheated) in the regenerator (State 4b) before being returned to the initial saturated liquid condition (State 1) in the condenser.

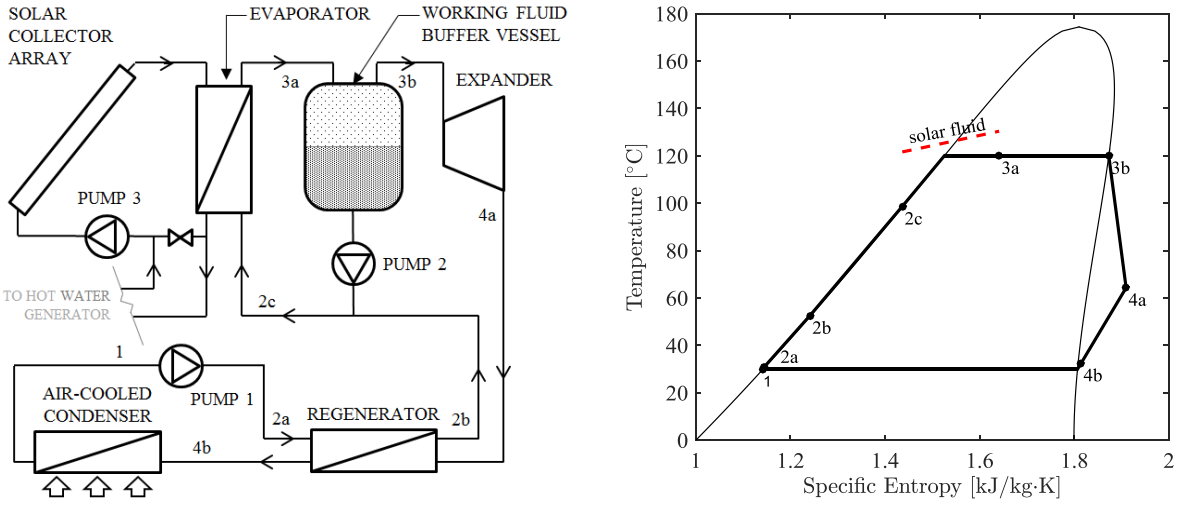

Figure 1: (a) Schematic diagram of the S-CHP system with a single-stage solar collector array; and (b) Temperature-entropy (*T*-*s*) diagram of the ORC with R245ca as the example working fluid.

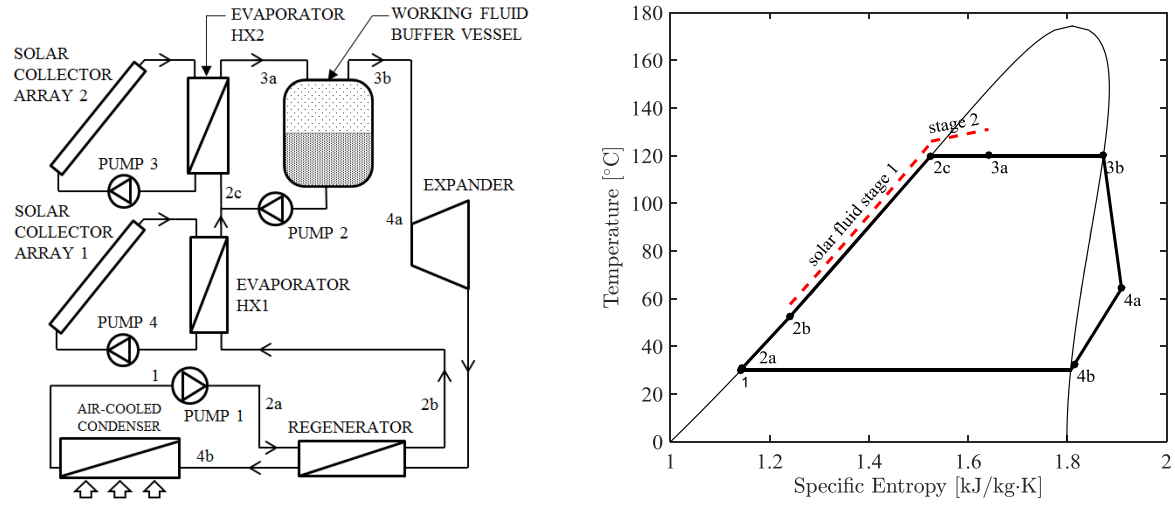

Figure 2: (a) Schematic diagram of the S-CHP system with two-stage solar collector array; and (b) Temperature-entropy (*T*-*s*) diagram of the ORC with R245ca as the example working fluid.

The benefits of the system design described are as follows: (1) the buffer vessel suppresses the variations in the expander inlet vapour quality due to the intermittency of the solar heat-source, so that periods of stable operation can be maintained for longer than for a system with no thermal/fluid store; (2) the design enables system operation with fixed flow-rates so that the pumps, expander and heat exchangers can operate at their design (best-efficiency) conditions; (3) the design enables a stable fluid temperature to be achieved at the evaporator outlet, which simplifies the task of identifying the optimal working fluid and evaporation temperature/pressure over the annual period in the chosen climate.

A variant of the aforementioned system will also be examined that incorporates a two-stage solar collector array, based on the configuration proposed by Jing *et al*. (2010). In the modified configuration shown in Figure 2, the ORC working fluid heat addition process is split into a separate sensible and latent stage, each served by a separate heat exchanger and dedicated section of the solar collector array (although the total collector array area remains the same as for the single-stage configuration). The sensible pre-heating stage occurs prior to mixing with the recirculated flow from the buffer vessel, and thus the two streams are closer together in temperature before mixing which is exergetically preferable. Furthermore, the lower average temperature of the solar collector circulating fluid in the first stage allows for a closer match in temperature between the fluid streams (illustrated by the red lines in Figure 2b), and a higher overall solar collector array efficiency. This configuration requires the inclusion of an additional pump and heat exchanger, the cost impact of which are discussed briefly in Section 3.3.

2.2 Solar collector array

The model of solar collector chosen for this study is the TVP SOLAR *HT-Power*, a high efficiency evacuated flat-plate collector highlighted for its potential in ORC applications in the study by Calise *et al.* (2015). The properties of the solar collector are listed in Table 1. In the aforementioned study, the diathermic oil DOWTHERM™ A (DOW, 1997) is chosen as an appropriate circulating fluid for this solar collector due to its temperature application range, and therefore the same fluid will be used for the simulations in the present work. The solar collector is modelled using the manufacturer's efficiency curve equation, where collector efficiency is expressed as a function of solar irradiance I_{sol}, ambient air temperature T_{a}, and mean solar collector temperature $\bar{T}_{\mathrm{sc}}$:

$$\eta_{\mathrm{sc}} = K_{\theta}\eta_0 - a_1 \cdot \frac{\bar{T}_{\mathrm{sc}} - T_{\mathrm{a}}}{I_{\mathrm{sol}}} - a_2 \cdot \frac{(\bar{T}_{\mathrm{sc}} - T_{\mathrm{a}})^2}{I_{\mathrm{sol}}} . \quad (1)$$

For the calculation of the overall solar collector array efficiency, a modified expression is required that takes into account the non-linear decrease in collector efficiency with fluid temperature. Thus Jing *et al*., (2010) derive the following expression for the collector array efficiency by integrating the

local collector efficiency over the total length of the array, provided that the inlet and outlet solar fluid temperatures ($T_{\mathrm{sf,in}}$, $T_{\mathrm{sf,out}}$) are known:

$$\eta_{\mathrm{sc,array}} = \frac{(a_2/I_{\mathrm{sol}})(\varphi_2-\varphi_1)\left[c_{\mathrm{p},0}\left(T_{\mathrm{sf,out}}-T_{\mathrm{sf,in}}\right)+0.5\alpha\left(T_{\mathrm{sf,out}}-T_{\mathrm{sc,in}}\right)\left(T_{\mathrm{sf,out}}+T_{\mathrm{sf,in}}-2T_{\mathrm{sf},0}\right)\right]}{\left[c_{\mathrm{p},0}+\alpha\left(T_{\mathrm{a}}-T_{\mathrm{sf},0}+\varphi_1\right)\right]\ln\left(\frac{T_{\mathrm{sf,out}}-T_{\mathrm{a}}-\varphi_1}{T_{\mathrm{sf,in}}-T_{\mathrm{a}}-\varphi_1}\right)+\left[c_{\mathrm{p},0}+\alpha\left(T_{\mathrm{a}}-T_0+\varphi_2\right)\right]\ln\left(\frac{\varphi_2-T_{\mathrm{sf,in}}+T_{\mathrm{a}}}{\varphi_1-T_{\mathrm{sf,out}}+T_{\mathrm{a}}}\right)}\,, \tag{2}$$

where $c_{\mathrm{p},0}$, α and T_0 are parameters that describe a linear variation of specific heat capacity with temperature for the solar heat-transfer fluid such that $c_{\mathrm{p,sc}} = c_{\mathrm{p},0} + \alpha\left(T_{\mathrm{a}} - T_{\mathrm{sf},0}\right)$, and parameters φ_1 and φ_2 are the solution values (negative and positive, respectively) of the quadratic function $\eta_0 - a_1\varphi/I_{\mathrm{sol}} - a_2\varphi^2/I_{\mathrm{sol}} = 0$. By assuming that the quantity of solar radiation absorbed by the collector array is equal to the enthalpy rise of the heat-transfer fluid:

$$\dot{Q}_{\mathrm{sf}} = \eta_{\mathrm{sc}}A_{\mathrm{sc}}I_{\mathrm{sol}} = (\dot{m}c_{\mathrm{p}})_{\mathrm{sf}}\left(T_{\mathrm{sc,out}} - T_{\mathrm{sc,in}}\right). \tag{3}$$

Finally, in order to calculate the pumping power required to circulate the solar fluid, pressure drops in the solar collector array are estimated using data provided by the manufacturer (see Table 1).

Table 1: System model parameters

Solar collector parameters(i)		**ORC parameters**	
η_0	0.82	η_{pump}, η_{exp}	0.65, 0.75
a_1, a_2	0.399, 0.0067	η_{gen}	0.90
$K_{\theta(\theta=50°)}$	0.91	ε_{r}	0.95
ΔP_{sc} (ii) (kPa)	0.7	T_{cond} (iii) (°C)	30

(i) Information taken from HT-Power product datasheet (TVP SOLAR, 1997) and Calise *et al*. (2015); (ii) at $\dot{V}_{\mathrm{ref}}$ = 51 L/m^2/hr; (iii) if $T_{\mathrm{sat}}(P_{\mathrm{atm}})$ > 30 °C, then $T_{\mathrm{cond}} = T_{\mathrm{sat}}(P_{\mathrm{atm}})$

2.3 Heat exchanger model

A finite element method is used to model the heat transfer process in the evaporator. The evaporator is modelled as a counterflow concentric-tube heat exchanger, with the ORC working fluid flowing inside the tube and the solar heat-transfer fluid flowing in the annulus. The heat exchanger length is divided into *N* finite elements, and the enthalpy and temperatures of the ORC working fluid and solar collector heat-transfer fluid for the $(n+1)^{\mathrm{th}}$ element are calculated from:

$$h_{\mathrm{wf},n+1} = h_{\mathrm{wf},n} + \frac{U\pi D_{\mathrm{i}}N_{\mathrm{tubes}}\left(T_{\mathrm{sf,n}}-T_{\mathrm{wf,n}}\right)}{\dot{m}_{\mathrm{wf}}}\Delta L\,, \tag{9}$$

$$T_{\mathrm{sf},n+1} = T_{\mathrm{sf},n} + \frac{U\pi D_{\mathrm{i}}N_{\mathrm{tubes}}\left(T_{\mathrm{sf,n}}-T_{\mathrm{wf,n}}\right)}{(\dot{m}c_{\mathrm{p}})_{\mathrm{sf}}}\Delta L\,, \tag{10}$$

where the total heat transfer coefficient between the fluid streams is $U = 1/(h_{\mathrm{c,i}}^{-1} + h_{\mathrm{c,o}}^{-1})$. Note that due to the counterflow arrangement of the heat exchanger, element $n = 1$ of the heat exchanger represents the working fluid inlet and the solar fluid outlet. The evaporator heat exchangers are approximately sized so that the "pinch-point" temperature difference between the fluid streams is $\Delta T_{\mathrm{pinch}} \approx 5$ K. The heat exchangers are sized with a suitable number of parallel tubes to achieve *Re* ≈ 3000 in the solar fluid stream. Local heat transfer coefficients in the single-phase and two-phase heat exchanger stages are calculated following the methods in Incropera *et al*. (2006) and Wang and Touber (1991). With both fluid flow rates and the working fluid evaporator inlet temperature supplied as input parameters, the working fluid outlet and solar fluid inlet and outlet temperatures are solved so that $(\dot{m}\Delta h)_{\mathrm{wf}} = -(\dot{m}\Delta h)_{\mathrm{sf}}$. Finally, the pressure drops in the evaporator heat exchangers are calculated using the Reynolds number/friction factor correlations in Incropera *et al.*, (2006).

2.3 ORC engine model

The power required by the ORC pump and power output of the ORC expander are calculated using

their respective isentropic efficiencies (see Table 1):

$$\dot{W}_{\mathrm{pump,1}} = \dot{m}_{\mathrm{pump1}}(h_{\mathrm{2a}} - h_1)/\eta_{\mathrm{pump}} \,, \tag{4}$$

$$\dot{W}_{\mathrm{exp}} = \eta_{\mathrm{exp}}\dot{m}_{\mathrm{pump1}}\left(h_{\mathrm{3b}} - h_{\mathrm{4a,s}}\right) \,, \tag{5}$$

where h_1 is the specific enthalpy of the working fluid as a saturated liquid at the condensation pressure, h_{3b} is the specific enthalpy of the working fluid as a saturated vapour at the evaporation pressure and η_{exp} is chosen to be broadly representative of a generalised small-scale positive-displacement expander (Freeman *et al*. 2015). The change in enthalpy of the working fluid in the regenerator heat exchanger is calculated using an effectiveness parameter ε_{r}:

$$h_{\mathrm{2b}} = h_{\mathrm{2a}} + \varepsilon_{\mathrm{r}}(h_{\mathrm{4a}} - h_{\mathrm{4b\prime}}) \,, \tag{6}$$

where $h_{\mathrm{4b\prime}}$ is the specific enthalpy of the working fluid at the condensation pressure and at the temperature $T_{\mathrm{4b\prime}} = T_{\mathrm{2a}}$. The net electrical power output from the ORC system is:

$$\dot{W}_{\mathrm{net}} = \eta_{\mathrm{gen}}\dot{W}_{\mathrm{exp}} - \dot{W}_{\mathrm{pump,1}} - \dot{W}_{\mathrm{pump,2}} - \dot{W}_{\mathrm{pumps,3\&4}} \,, \tag{7}$$

2.4 Fluid flow rates

The mass flow-rate of ORC working fluid circulated by pumps 1 and 2 is maintained at a fixed ratio of 1:2 such that $\dot{m}_{\mathrm{pump2}} = 2 \cdot \dot{m}_{\mathrm{pump1}}$. The solar heat transfer-fluid flow-rate circulated by Pump 3 is set for a temperature glide of ΔT_{sf} = 5 K between the solar fluid inlet and the pinch point corresponding to the working fluid bubble point, for a design condition in which the vapour quality at the evaporator outlet x_{3a} = 0.33. Thus:

$$\dot{m}_{\mathrm{pump3}} = \left(\dot{m}_{\mathrm{pump1}} + \dot{m}_{\mathrm{pump2}}\right)(h_{\mathrm{3a}} - h_{\mathrm{bubble}})/c_{\mathrm{p,sf}}\Delta T_{\mathrm{sf}} \,, \tag{8}$$

For the two-stage collector configuration, the mass flow-rate circulated by Pump 4 is sized by a similar method as above to achieve an approximately parallel temperature glide between two fluid streams in the first stage heat exchanger, as shown in Figure 2b.

2.5 Working fluid buffer vessel

As mentioned earlier in Section 2.1, the presence of the buffer vessel at the evaporator outlet ensures that the working fluid always enters the expander as a saturated vapour at the chosen cycle evaporation temperature. Heat transfer in the buffer vessel is not treated in detail in this work. Following the approach of Jing *et al*. (2010), the buffer vessel is assumed to be perfectly insulated, zero-dimensional and of sufficient size to provide the required buffering for stable performance of the system over the entire annual period. Thus for each time-step of the annual simulation, the change in internal energy of the total fluid mass in the buffer vessel is:

$$\Delta U_{\mathrm{bv}} = \left[\left(\dot{m}_{\mathrm{pump1}} + \dot{m}_{\mathrm{pump2}}\right)h_{\mathrm{3a}} - \dot{m}_{\mathrm{pump1}}h_{\mathrm{3b}} - \dot{m}_{\mathrm{pump2}}h_{\mathrm{bubble}}\right]\Delta t \,. \tag{11}$$

2.6 Annual simulations

For the annual assessment, the system performance is evaluated using London, UK annual climate data comprised of hourly solar irradiance and air temperature values (ASHRAE, 2001). An optimal tilt angle is chosen for the solar collector array in order to maximise the annual solar irradiation received (the optimal tilt angle calculated using the climate data set is found to be 40.5° for a due south orientation). The ORC system is operational during all hours in which the climatic conditions (solar irradiance and ambient air temperature) are sufficient such that $\eta_{\mathrm{sc}} > 0$. During these hours, the ORC expander operates under constant flow-rate and power output conditions. If $h_{\mathrm{3a}} > h_{x=0.33}$, then heat (enthalpy) is stored in the buffer vessel while if $h_{\mathrm{3a}} < h_{x=0.33}$ then heat (enthalpy) is released from the buffer vessel. The area of the solar collector array is fixed at A_{sc} = 15 m^2 (Freeman *et al*.,

2015a) and the fixed value for the mass flow-rate of Pump 1 is solved so that the net annual enthalpy gain by the buffer vessel is zero $\left(\sum_{hr=1}^{8760} \Delta H_{\mathrm{bv}} = 0\right)$. This procedure is repeated for each working fluid over the range of evaporation temperatures. The overall efficiency of the system operating over the annual period is evaluated as follows:

$$\eta_{\mathrm{overall}} = \sum_{hr=1}^{8760} \dot{W}_{\mathrm{net}} \,/\, \sum_{hr=1}^{8760} I_{\mathrm{sol}} A_{\mathrm{sc}} \,. \tag{12}$$

The exergy efficiency of the system can be evaluated as the net annual work output from the ORC engine divided by maximum convertible work (or exergy) output from the solar collector array operating at its optimum temperature and flow-rate at each time-instant:

$$\eta_{\mathrm{exergy}} = \sum_{hr=1}^{8760} \dot{W}_{\mathrm{net}} \,/\, \sum_{hr=1}^{8760} \dot{X}_{\mathrm{sc,out,max}} \,. \tag{13}$$

Following the approach in Freeman *et al.* (2015b), the flow-rate of exergy in the fluid stream leaving the collector is calculated as the integral of the power produced by an infinite number of infinitesimal Carnot engines operating between the hot stream and the cold reservoir (in this case the ambient air), resulting in the following equation:

$$\dot{X}_{\mathrm{sc,out}} = \eta_{\mathrm{sc}} A_{\mathrm{sc}} I_{\mathrm{sol}} \left[\left(1 - \left(T_{\mathrm{sc,out}} / T_{\mathrm{a}} - 1 \right) \right)^{-1} \ln\left(T_{\mathrm{sc,out}} / T_{\mathrm{a}} \right) \right]. \tag{14}$$

3. RESULTS AND DISCUSSION

3.1 Comparison of working fluids under steady-state conditions for single-stage system

In order to understand how the optimum choice of working fluid and evaporation temperature/pressure varies with solar irradiance, the single-stage system is simulated under steady-state conditions. A range of hydrocarbon (HC), hydrofluorocarbon (HFC), hydrochlorfluorocarbon (HCFC) and chlorofluorocarbon (CFC) refrigerants are chosen that have been investigated in previous works on low temperature and solar ORC systems (Chen *et al.* 2010; Rayegan and Tao, 2011; Bao and Zhao 2013). Figure 3 shows the simulated power output from the system at a low irradiance level (150 W m^{-2}) and a high irradiance level (800 W m^{-2}), for the different working fluids considered herein and over a range of evaporation temperatures. For each irradiance level and working fluid the evaporation temperature is varied in finite increments and the system flow-rates are solved for a steady-state operation (corresponding to a vapour quality at State 3a of x_{wf} = 0.33, such that $\Delta H_{\mathrm{bv}} = 0$). The resulting power output curves can then be used to identify the evaporation temperature that delivers maximum power output under steady-state irradiance conditions for each working fluid.

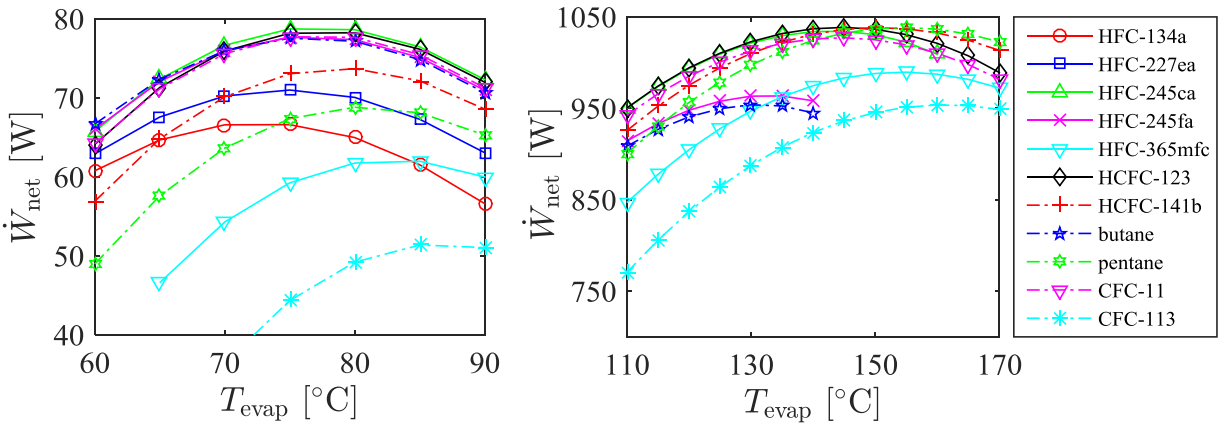

Figure 3: ORC net power output as a function of the evaporation temperature for conditions: (a) I_{sol} = 150 W m^{-2} and T_{a} = 20 °C; and (b) I_{sol} = 800 W m^{-2} and T_{a} = 20 °C.

It can observed in Figure 3 that the highest net power outputs for both the low and high irradiance condition are obtained with the fluids R245ca, R123 and R11. Furthermore, these fluids are found to perform well across a broad range of evaporation temperatures. The maximum net power output at the low irradiance level is 79 W (for working fluid R245ca), and is achieved at an ORC evaporation temperature of 78 °C. The maximum net power output at the high irradiance level is 1039 W (for working fluid R123) and is achieved at an ORC evaporation temperature of 144 °C. The corresponding solar collector array outlet temperatures in the low and high irradiance cases are 88 °C and 155 °C respectively. In both cases this is lower than the collector outlet temperatures corresponding to maximum exergy (calculated in Eq. 16), which are found to be 101 °C and 210 °C respectively. It can also be noted that the critical temperatures for most of the working fluids investigated (with the exception of R113 and R141b) are below 200 °C, and that this may restrict the attainable exergy efficiency of the system under higher irradiance conditions.

3.3 Comparison with two-stage system

For the following analysis, R245ca is chosen as the ORC working fluid of interest due to its favourable performance in the previous analysis and lower ozone depletion potential than R11 and R123. However, it should also be noted that at present R245ca is not widely available for purchase in bulk quantities in the UK. The steady-state simulations are repeated for the two-stage collector array configuration and the results compared with those for the single-stage configuration. For each steady-state condition, the system flow-rates and the relative areas of the first and second-stage collector arrays are solved so that the ORC working fluid leaves the first heating stage as a saturated liquid and the second heating stage as a two-phase fluid at the target vapour quality of $x_{\mathrm{wf}} = 0.33$ (illustrated by the *T*-*s* diagram in Figure 2b). The results are compared to the single-stage configuration in Figure 4. For the two-stage configuration the system is found to operate with a higher overall collector array efficiency, and the result is a 5% increase in maximum net power output in the low irradiance case and a 7% increase in maximum net power in the high irradiance case. It can also be observed that the peak power output for the two-stage configuration occurs at a higher evaporation temperature than for the single-stage configuration. This is most evident in the high irradiance case, for which the peak power output occurs at an evaporation temperature of 155 °C for the two-stage configuration compared to 144 °C for the single-stage configuration. For the two-stage system the ratio of the first-stage collector array area to total collector array area (also shown in Figure 4 on the right-hand *y*-axis) is found to increase with evaporation temperature. This can be easily understood by the increased ratio of sensible heating to latent heating of the Rankine cycle working fluid as evaporation temperature is increased. With the addition of the second stage heat exchanger, the overall heat transfer area increases by 42%. Taking this additional heat exchanger cost into account and also considering the need for the additional pump, the expected cost increase of the two-stage system relative to the single-stage system is in the region of €450-500. Thus the increase in system cost per additional Watt of nominal power output is approximately 6 €/W.

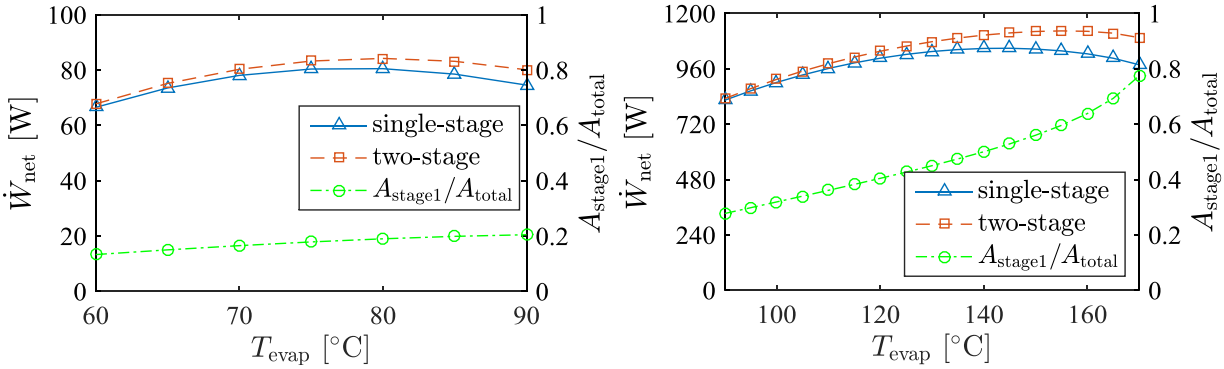

Figure 4: Comparison of the ORC net power output from single-stage and two-stage solar collector configurations (with the relative array areas of the two-stage configuration also shown), with R245ca as the working fluid and for conditions: (a) I_{sol} = 150 W m^{-2} and T_{a} = 20 °C; and (b) I_{sol} = 800 W m^{-2} and T_{a} = 20 °C.

Table 2: Results from the simulations of the annually optimised system with single-stage and two-stage collector configurations

Parameter	**Unit**	**Single-stage collector configuration**	**Two-stage collector configuration**
Optimal ORC working fluid	-	R245ca	R245ca
Optimal ORC evaporation temperature	°C	117	126
Solar collector array area (Stage 1 / Stage 2)	m^2	15 m^2	6.3 m^2 / 8.7 m^2
Net annual work output	kWh yr^{-1}	955	1070
Annually averaged net power output	W	109	122
Instantaneous/nominal net power output	W	403	481
Hours operational	hr yr^{-1}	2372	2227
Mean solar collector array efficiency	-	44.0%	46.5%
ORC electrical efficiency	-	12.8%	13.6%
Annual overall efficiency	-	5.6%	6.3%
Annual exergy efficiency	-	52.2%	58.5%

3.2 Annual simulation of single-stage and two-stage system

The S-CHP system is simulated over an annual period with UK climate data for both the single-stage and two-stage solar collector array configurations and with R245ca as the working fluid. The ORC evaporation temperature and the relative sizes of the solar collector arrays (in the two-stage configuration) are optimised to deliver the highest net annual electrical work output from the system, and the results for the optimum settings are presented in Table 3. It is found that the system with the two-stage collector array configuration is able to deliver a 12% higher net annual work output than the single-stage system. The optimal ORC evaporation temperature is also found to be 9 °C higher for the two-stage system, resulting in a 19% increase in instantaneous power output from the ORC; however the higher temperatures in the system also result in a larger number of hours (under very low irradiance conditions) for which $\eta_{sc} \leq 0$, and therefore the total number of operational hours per year is reduced.

The maximum annual work output reported here is also found to be 53% higher than that in our earlier work (Freeman *et al*., 2015a). The improvement can be specifically attributed to the various system modifications that have been made, as follows: (i) ~4% improvement due to the choice of working fluid; (ii) ~10% improvement due to the choice of solar collector module; (iii) ~8% improvement due to the addition of the regenerator heat exchanger; and (iv) ~12% improvement due to the two-stage collector array configuration. The remaining improvement (a further ~20%) in power output can be attributed to the manner in which the system was simulated and optimised, specifically; the use of monthly aggregated climate data in the prior work was found to result in a non-trivial reduction in calculated power output due to non-linearity in the relationship between solar irradiance and system power output, whereas in the present analysis, the peaks in solar irradiance are more effectively represented by the hourly resolution dataset.

4. FURTHER DISCUSSION AND CONCLUSIONS

A study of a domestic-scale solar combined heat and power (S-CHP) system has been undertaken in order to assess its electrical performance in a London UK setting. Challenges for the design and operation of the system and its components due to the intermittent nature of the UK solar resource were addressed by incorporating a working fluid buffer vessel, hypothetically sized to enable year-round operation. Thus, the system can be operated with fixed fluid flow-rates, limiting losses in component efficiencies due to part-load operation and enabling continuous power output for longer periods.

Of the range of working fluids investigated, R245ca was found to result in the highest net annual work output for the basic single-stage system design, which was 955 kWh yr^{-1} (64 kWh yr^{-1} per m^2 of solar collector) at a cycle evaporation temperature of 117 °C. This is equivalent to a continuous power output of 109 W when averaged over the whole year. A modified design incorporating a two-stage solar

collector array was found to offer a further 12% in annual work output (1070 kWh yr^{-1}, or 71 kWh yr^{-1} per m^2), due to the improvement in overall collector array efficiency. In the present design the two-stage collector array requires an additional pump and heat exchanger and therefore an associated increase in capital cost of the system; however future work will explore the possibility of directly heating the ORC working fluid in the solar collector, thus omitting the need for the secondary fluid circuit.

The results presented here suggest that the S-CHP system operating in a UK setting can be expected to provide in the region of 32% of the typical household demand for electricity (3300 kWh yr^{-1} according to OFGEM, 2011). While significant, this is still found to be less than half of the predicted electrical output for the same system when simulated in a southern European climate. The electrical performance can be compared to that of a mono-crystalline PV system which typically provides 110-120 kWh m^{-2} yr^{-1} in the UK climate (The Energy Saving Trust, 2011a), and thus for an equivalent array size (15 m^2) approximately 50% of household demand. The advantage of the S-CHP system design discussed here is the ability to also provide water heating and to store thermal energy during times of low electricity demand for better load profile matching, as well as a considerably lower capital expenditure (by at least one-third, and arguably up to one-half). However, overall system performance also depends on well-designed solar collectors, able to operate with high efficiency at high fluid temperatures while also making use of the large proportion of diffuse (scattered) radiation received in the UK. The new generation of evacuated flat-plate solar collector investigated here is a strong candidate technology for such an application.

Finally, it is emphasised that this paper has focused on the performance of the S-CHP system when optimised for maximum annual electrical power generation. In CHP operation, a proportion of the solar collector heat transfer fluid may be diverted to a domestic hot water cylinder (see the system schematic in Figure 1a), at the expense of a reduction in the thermal input to the ORC engine. Taking the water heating demand for a typical UK home to be around 2900 kWh yr^{-1} (The Energy Saving Trust, 2011a), the reduction in the annual electrical output from the S-CHP system in order to meet this heating demand can be expected to be in the region of 35-45%.

NOMENCLATURE

A	area	(m^2)
η_0, a_1, a_2	solar collector efficiency curve parameters	(–)
h	specific enthalpy	(J kg^{-1})
h_c	convective heat transfer coefficient	(W m^{-2} K^{-1})
I_{sol}	solar irradiance	(W m^{-2})
K_θ	solar collector incident angle modifier	(–)
$\dot{m}$	mass flow-rate	(kg s^{-1})
P	pressure	(Pa)
s	specific entropy	(J kg K^{-1})
T	temperature	(°C)
t	time	(s)
U	overall heat transfer coefficient	(W m^{-2} K^{-1})
x	vapour quality	(–)
ε	heat exchanger effectiveness	(–)
η	efficiency	(–)
W	work	(W)

Subscript

a	ambient air
bv	working fluid buffer vessel
bubble	bubble-point (saturated liquid condition)
exp	expander
gen	generator
i, o	inner, outer

in, outer	inlet, outlet
r	regenerator
s	isentropic process
sc, sf	solar collector, solar collector circulating fluid
wf	ORC working fluid
1,2,3…	cycle state points

REFERENCES

ASHRAE, 2001, International Weather for Energy Calculations (IWEC Weather Files) Users' Manual and CD-ROM, Atlanta. Available from: <apps1.eere.energy.gov/buildings/energyplus/cfm/weather_data.cfm> [accessed 24/2/2015].

Bao, J., Zhao, L., 2013, A review of working fluid and expander selections for organic Rankine cycle, *Renew. Sustain. Energy Rev.*, vol. 24: p. 325–342.

Canada, S., Cohen, G., Cable, R., Brosseau, D., Price, H., 2004, Parabolic trough organic Rankine cycle solar power plant, *Solar Energy Technologies Program Review Meeting*, Denver, Colorado.

Calise, F., D'Accadia, M.D., Vicidomini, M., Scarpellino, M., 2015, Design and simulation of a prototype of a small-scale solar CHP system based on evacuated flat-plate solar collectors and Organic Rankine Cycle, *Energy Convers. Manag.*, vol. 90: p. 347–363.

Chen, H., Goswami, D.Y., Stefanakos, E.K., 2010, A review of thermodynamic cycles and working fluids for the conversion of low-grade heat, *Renew. Sustain. Energy Rev.*, vol. 14 no. 9: p. 3059–3067.

Dow, 1997, Dowtherm A Heat Transfer Fluid product technical data. Available from: <http://msdssearch.dow.com/PublishedLiteratureDOWCOM/dh_0030/0901b803800303cd.pdf?filepath=/heattrans/pdfs/noreg/176-01337.pdf&fromPage=GetDoc> [accessed 24/2/2015]

The Energy Saving Trust, 2011, A buyer's guide to solar electricity panels.

The Energy Saving Trust, 2011, Here comes the sun: a field trial of solar water heating systems.

Freeman, J., Hellgardt, K., Markides, C.N., 2015, An assessment of solar-powered organic Rankine cycle systems for combined heating and power in UK domestic applications, *Appl. Energy*, vol. 138: p. 605–620.

Freeman, J., Hellgardt, K., Markides, C.N., 2015, An assessment of solar-thermal collector designs for small-scale combined heating and power applications in the United Kingdom, *Heat Transf. Eng.*, vol. 36, no. 14–15: p. 1333–1348.

Incropera, F.P., DeWitt, D.P., Bergman, T.L., Lavine, A.S., 2006, *Fundamentals of Heat and Mass Transfer*, sixth ed., John Wiley & Sons, New Jersey.

Jing, L., Gang, P., Jie J., 2010, Optimization of low temperature solar thermal electric generation with Organic Rankine Cycle in different areas, *Appl. Energy*, vol. 87: p. 3355–3365.

Manolakos, D., Kosmadakis, G., Kyritsis, S., Papadakis, G., 2009, On site experimental evaluation of a low-temperature solar organic Rankine cycle system for RO desalination, *Sol. Energy*, vol. 83: 646–656.

OFGEM (Office of Gas and Electricity Markets), 2011, Typical domestic energy consumption figures factsheet, Available from: <https://www.ofgem.gov.uk/ofgem-publications/76112/domestic-energy-consump-fig-fs.pdf> [accessed 24/2/2015].

Quoilin, S., Orosz, M., Hemond, M., Lemort, V., 2011, Performance and design optimization of a low-cost solar organic Rankine cycle for remote power generation, *Sol. Energy* vol. 85: p. 955–966.

Rayegan, R., Tao, Y. X., 2011, A procedure to select working fluids for Solar Organic Rankine Cycles (ORCs), *Renew. Energy*, vol. 36, no. 2: p. 659–670.

TVP Solar, 2013, HT-Power Product datasheet. Available from: <http://www.tvpsolar.com/files/pagine/HT-Power%20Datasheet%20(v4.2x)(ver3).pdf> [accessed 24/2/2015].

Wang H. and Touber S., 1991, Distributed and non-steady-state modelling of an air cooler, *Int. J. Refrig.*, vol. 14, no. 2: p. 98–111.

Wang, X.D., Zhao, L., Wang, J.L., Zhang, W.Z., Zhao, X.Z., Wu, W., 2009, Performance evaluation of a low-temperature solar Rankine cycle system utilizing R245fa, *Sol. Energy*, vol. 84: p. 353–364.